Mechatronic Design and Active Disturbance Rejection Control of a Bag Valve-based Mechanical Ventilator

Jaime Arcos-Legarda
Full Professor
Department of Mechatronics Engineering
Universidad de San Buenaventura
Bogotá, Colombia
Email: warcos@usbbog.edu.co

Andres Tovar
Associate Professor
Department of Mechanical and Energy Engineering
Indiana University-Purdue University Indianapolis
Indianapolis, Indiana, USA
Email: tovara@iupui.edu

ABSTRACT

This paper presents the mechatronic (mechanical and control system) design of a functional prototype of a portable mechanical ventilator to treat patients with a compromised respiratory function. The portable ventilator ensures adequate oxygenation and carbon dioxide clearance while avoiding ventilator-induced lung injury (VILI). Oxygen is delivered through the compression of a bag valve (Ambu bag) using a moving strap. Carbon dioxide is cleared through the control of a pinch valve actuated by a low-torque servo motor. The positive end expiratory pressure (PEEP) is controlled by an adjustable mechanical valve the system. An Arduino Mega microcontroller board is used in this prototype to control the respiratory variables. All mechanical components as well as sensors, actuators and control hardware are of common use in robotics and are very inexpensive. The total cost of the prototype build in this work is about $425 U.S. dollars. The design is meant to be replicated and utilized in emergency conditions that involve an overwhelming number of cases, such as COVID-19 treatment, in places with no access to commercial MV technologies. In order to account for variations in the prototype as built, the software developed for this portable MV applies an active disturbance rejection control strategy (ADRC). This control strategy is presented as a universal control structure for any mechanical ventilator able to supply air flow with controlled pressure and volume.

This is the author's manuscript of the article published in final edited form as:
Arcos-Legarda, J., & Tovar, A. (2021). Mechatronic Design and Active Disturbance Rejection Control of a Bag Valve-Based Mechanical Ventilator. Journal of Medical Devices, 15(3). https://doi.org/10.1115/1.4051064

1 Introduction

1.1 Mechanical ventilation

Mechanical ventilation (MV) is a life-sustaining medical procedure that supports or replaces the normal, spontaneous breathing of a patient. MV is utilized in the treatment of patients with acute respiratory distress syndrome (ARDS), compromised lung function, or breathing difficulty due to pathological changes to the respiratory system and/or pulmonary tissue [1]. In the U.S., more than half of the patients (53% [CI: 52.2-53.9%]) are provided MV when admitted to intensive care units (ICUs) [2]. It is estimated that 2.7 per 1,000 population per year are mechanically ventilated during hospitalization [3], with a mean length of stay of 14.1 days (7.1% of hospital days) [4]. It can be projected that about 894,000 patients will use MV during hospitalization in 2020 under normal circumstances. With more than 25 million confirmed COVID-19 cases in the U.S. [5], this number is expected to increase significantly.

The primary function of MV is to assist lung oxygenation and carbon dioxide clearance from the blood passing through their capillary network. Different ventilation modes and settings can be provided depending on tidal volume (TV), plateau pressure (Pplat), partial pressure of arterial oxygen (PaO2) or oxyhemoglobin saturation (SpO2), percentage of inspired oxygen (FiO2), partial pressure of carbon dioxide (PaCO2), positive end-expiratory pressure (PEEP), peak inspiration pressure (PIP), respiratory rate (RR), and inspiratory/expiratory time ratio (I/E ratio) [6]. To avoid ventilator-induced lung injury (VILI), the general principles of ARDS management with ventilatory supportive care include an initial TV of 6 mL/kg based on predicted body weight of the patient, Ppla under 30 mm Hg (Ppla over 35 mm Hg has been correlated with risk of barotrauma), PaO2 of 55 to 80 mm Hg or SpO2 of 88 to 95%, and FiO2 under 60% (for a normal person breathing room air, FiO2 is about 21%) [7]. A normal I/E ratio in MV is usually around 1:2 with a RR of 8 to 12 breaths per minute for patients not requiring hyperventilation [8]. During controlled ventilation, expiratory time is prolonged (I/E ratio 1:3 or greater) with RR of 10 to 15 breaths per minute [9]. The PEEP has protective effects on the lungs during mechanical ventilation diminishing the probability of edema and preventing the risk of alveolar collapse or flooding during intermittent positive pressure ventilation with high tidal volume [10]. Due to their control versatility, MV parameters can be set to treat COVID-19 patients who show ARDS-like symptoms.

1.2 Mechanical ventilator design

A typical mechanical ventilator includes a power source, an oxygen and air supply, a gas mixer, a flow/pressure generator, a breathing system, a humidifier, and an expiratory valve. ICU ventilators are supplied with oxygen and air via a central gas system with supply pressures in the range of 3 to 6 bar. These ventilators run on AC power and contain a back-up battery in the event of power failure. Transport ventilators, available in ambulances, utilize compressors and compressed gas cylinders. These ventilators can be powered pneumatically or using electric (AC or DC) energy. High performance ventilators are electrically powered. Increasingly, all ventilators use filtered ambient air, so only an oxygen source and an electric power supply are required.

The gas mixer allows to set FiO2 from 21 to 100% by controlling two valves: compressed air and oxygen valves. Usually, the gas mixer also controls the TV and peak inspiratory flow rate of the mixed gas. Most modern ventilators

can deliver flow rates between 60 and 120 L/min (in most patients, peak flow rates of 60 L/min are adequate) [11]. The flow/pressure generator delivers the mixed gas to the breathing system in one of two ways: as a flow generator (uncontrolled pressure) or as a pressure generator (uncontrolled flow). In other words, in order to achieve a set TV, a flow generator adjusts the flow rate while the pressure generator adjusts the flow pressure. TV can usually be set in the range of 200 to 800 mL. RR can be adjusted between 6 and 40 breaths per minute. I/E Ratio is adjustable between 1:1 to 1:4.

The breathing system is the interface between the patient and the ventilator. Usually, the breathing system is a dual-hose circuit formed by an inspiratory hose and an expiratory hose. The gas delivered through the inspiratory hose passes through a gas humidifier before entering the patient's lungs. The gas humidifier warms and humidifies the inspiratory gas. After the inspiratory phase, the expiratory phase initiates when an exhalation valve opens. If the exhalation valve is not opened completely, a PEEP is created in lungs. PEEP of 5 to 15 cm H20 is therapeutically important as it increases gas exchange surface in the lungs and also prevents collapse of alveolar areas. The exhalation valve is also controlled during the inspiration phase to compensate for undesired rises in pressure caused, for example, by patients' coughing.

1.3 Mechanical ventilator manufacturers and types

The major manufacturers of ICU ventilators are Getinge (Sweden), Hamilton Medical (USA and Switzerland), and Drager (Germany) with global market shares of 22%, 22%, and 15%, respectively (Source: IPG Research [12]). The cost of an ICU ventilator is about $25,000 U.S. dollars. The major manufacturers of transport ventilators are Drager (Germany), Weinman Medical (Germany), and Hamilton Medical (USA and Switzerland) with global market shares of 24%, 21%, and 18%, respectively (Source: IPG Research [12]). The average cost of a pneumatic transport ventilator is $1,000, while the average cost of an electric transport ventilator is $5,000.

An alternative to ICU and transport ventilators are manual disposable resuscitators produced by companies such as Ambu (Denmark) and Laerdal (Norway). The manual resuscitators, also called bag-valve masks (BVMs) or Ambu bags, are hand-held devices that provide ventilation using a self-inflating bag. The use of BVMs provides a low-cost solution, at a fraction of the cost of a transport ventilator. An Ambu bag costs about $50 U.S. dollars.

A patent of a device incorporating a bag valve for manipulating intrathoracic pressures for the treatment of hypotension, head trauma, and cardiac arrest is currently active (U.S. patent US7275512B2 by Zoll Medical Corp.). The main limitation of the use of a bag valve is the need for manual operation. An Ambu-bag automation system has been patented (U.S. patent US20110041852A1 by Mobile Airways, LLC). Currently, there is a number of open-source solutions incorporating actuators, instrumentation, and control systems on bag valves. The resulting functional prototypes of bag valve-based MVs hold the promise to be inexpensive—under $1,500 U.S. dollars [13], under $500 U.S. dollars [14], or under under $200 U.S. dollars [15]. An additional benefit of bag valve-based ventilators is to prevent or alleviate a potential collapse of pressure lines in hospitals due to a sudden increased need for mechanical ventilators.

Despite their potential benefit, there are several concerns about the use of low-cost, bag valve-based ventilators. Such ventilators may not be reliable when operating during extended periods of time. Mechanical and electrical components may fail, jeopardizing the ventilator's ability to maintain the settings required by the clinician and, therefore, making it unable to

provide a proper ventilation. Improper ventilation may induce lung injuries such as lung overdistension (volutrauma) [16], overpressure within distal airways and alveoli (barotrauma) [17], and repeated alveolar collapse and expansion (atelectrauma) [18, 19, 20, 21]. The respiratory settings in an invasive mechanical ventilation are a key factor to avoid additional lung injury. A common sense is to avoid high pressure of tidal volume; however, extremely low ventilation, with ultra-protective ventilation methods, may be associated with undesired effects such as hypoxemia [22, 23]. Therefore, a robust, certified, and well tested system is required before considering the clinical use of a mechanical ventilator.

1.4 Purpose of this work

In this work, a functional prototype of a bag valve-based mechanical ventilator has been designed, fabricated, and tested. The proposed mechanical ventilator has very few mobile parts, which makes its design simple and reliable. In contrast to most bag valve-based mechanical ventilators, which use rigid elements to compress the bag, the proposed design uses a flexible strap that conforms around the bag making the operation smoother. In order to reduce the concerns associated with the use of bag valve-based mechanical ventilators, the proposed design incorporates an active disturbance rejection control (ADRC) strategy. The ADRC is a model-based, robust control approach that attenuates the effect of model uncertainties as well as random internal disturbances attributed to loss of mechanical stability (e.g., strap distension, misalignment) and random external disturbances attributed to breathing irregularities. Without a proper rejection, such uncertainties and disturbances would significantly affect the proper operation of the ventilator. The ADRC strategy has been successfully utilized in the control of walking robots [24]. The implementation in a low-cost, bag valve-based mechanical ventilator design is described in this paper.

This paper is organized as follows: The mechanical design of the bag valve-based mechanical ventilator is described in Sec. II. This includes the design of the mechanical systems and the selection of sensors, actuators, and control hardware. The control strategies (finite-element machine and active disturbance rejection control) are described in Sec. III. Finally, the results of experimental tests and conclusions are presented in Secs. IV and V, respectively.

2 Mechatronic Design

2.1 Bag valve compression mechanism

According to the compressing element, compression mechanisms in bag valve-based ventilators can be classified into rigid and flexible. Ventilators with a *rigid* compressing element squeeze the bag using two or more rigid elements. In this type of ventilators, the compressing elements may have flat or curved shapes. These elements can be moving or stationary. The moving elements can rotate around a pivot or reciprocate along a linear guide. Ventilators with a *flexible* compressing element squeeze the bag using at least one non-rigid element. Examples include the use of a squeezable bladder and straps. External compressed air can also be utilized to squeeze the bag.

Most of the open-source, bag valve-based ventilators use a rigid compressing element. Configurations include the use of a single pivoting, curved element squeezing the bag against a stationary flat element [14], two pivoting flat elements squeezing a simply supported bag [25], one linear reciprocating actuator squeezing the bag against a stationary flat element

[13, 15, 26], two linear, reciprocating actuators squeezing a simply supported bag [27], and two pivoting curved elements compressing a bag supported on a flat bed [28]. Less common is the use of flexible elements.

There are several reasons why rigid compressing elements are traditionally selected. First, rigid elements can be made using laser-cut or 3D-printed plastic or metal. This allows to share files online and make the design highly reproducible. Second, the operation of the rigid elements is highly predictable, which improves the controlability of the ventilator. Third, the designs are compact. However, the use of a flexible element, such as a strap, offers several benefits. First, flexible elements could produce minor damage to bag. Second, the designs are less dependent on manufactured elements, reducing the need for a laser cutter or a 3D printer. Third, the mass of the flexible element is substantially lower than the mass of rigid elements, which makes for a lighter design. Fourth, the strap can be made from a large variety of synthetic and natural fabrics or leather, which makes the design more accessible even in the absence of plastic or metal. In this work, the proposed design is a strap-based, bag-valve ventilator (Figs. 1 and 2). In this design, the strap wraps around the bag and around a pivot roller. The pivot rotates around a fixed axle located below the bag. The fixed end of the strap is attached to a fixed pin on the opposite side of the bag. The moving end of the strap is attached to a rotating wheel below the roller. The rotating wheel can be actuated by a stepper motor or a DC geared motor. Both configurations were tested in this work (see Sec. IV).

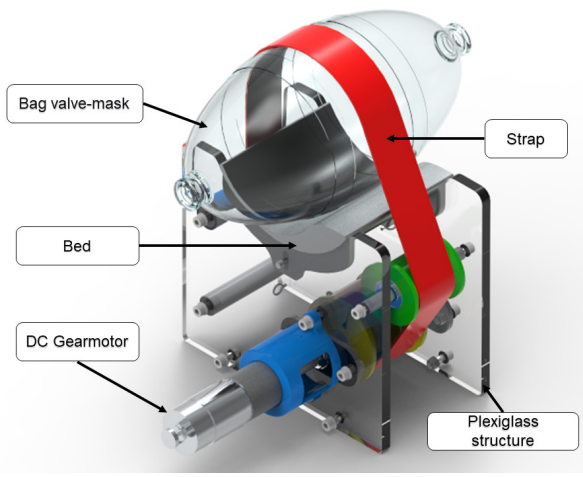

Fig. 1. Render of the mechanical ventilator design.

The housing structure is made of two plates made of acrylic—poly(methyl methacrylate). The bag valve is located between the plates and supported by a rigid bed covered by an elastomer. The elastomer conforms to the shape of the bag and prevents sliding. The two rolling elements (pivot and wheel) are supported by deep-groove ball bearings. Spacers and the shafts are made of steel. The total number of mechanical parts is 22 and the overall dimension is 25×25×25 cm and the total weight is 3.5 kg. The bill of materials of all structural components is included in the appendix.

2.2 Sensors, actuators, and control hardware

The control system is set by five parameters: tidal volume (TV), peak inspiration pressure (PIP), respiratory rate (RR), inspiratory/expiratory time ratio (I/E ratio), and positive end expiratory pressure (PEEP) (Table 1). Depending on the specific

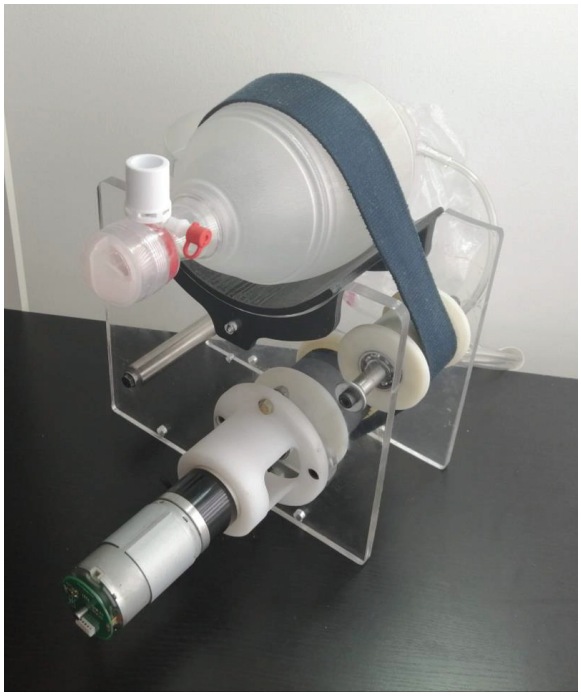

Fig. 2. Physical prototype of the mechanical ventilator.

patient treatment, the ventilator provides assist-control and mandatory-control for two control variables: pressure (PIP) and volume (TV). PIP is measured by a piezoresistive silicon pressure sensors and controlled with the pressure output produced by the compression of the bag valve. This pressure is proportional to the electrical current passing through the the DC geared motor (Sec. 3.2.2).TV is determined from the gas flow using Boyle's law. The gas flow is measured with a differential pressure sensor and a pitot tube. The control is provided through the compression of the bag valve utilizing an encoder attached to the DC geared motor (Sec. 3.2.3). RR and I/E ratio are controlled using an internal digital clock, which is implemented in an Arduino Mega 2560 Rev 3 microntroller. PEEP is mechanically setup and not integrated into the closed loop control. The set of parameters in the mechanical ventilator with their range are provided in Table 1.

Table 1. Parameters

Parameter	Symbol	Range
Tidal volume	TV	200 to 600 mL
Peak inspiration pressure	PIP	5 to 40 cmH2O
Respiratory rate	RR	0 to 30 bpm
Inspiratory/expiratory time ratio	I/E ratio	1:1 to 1:3
Positive end expiratory pressure	PEEP	5 to 20 cmH2O

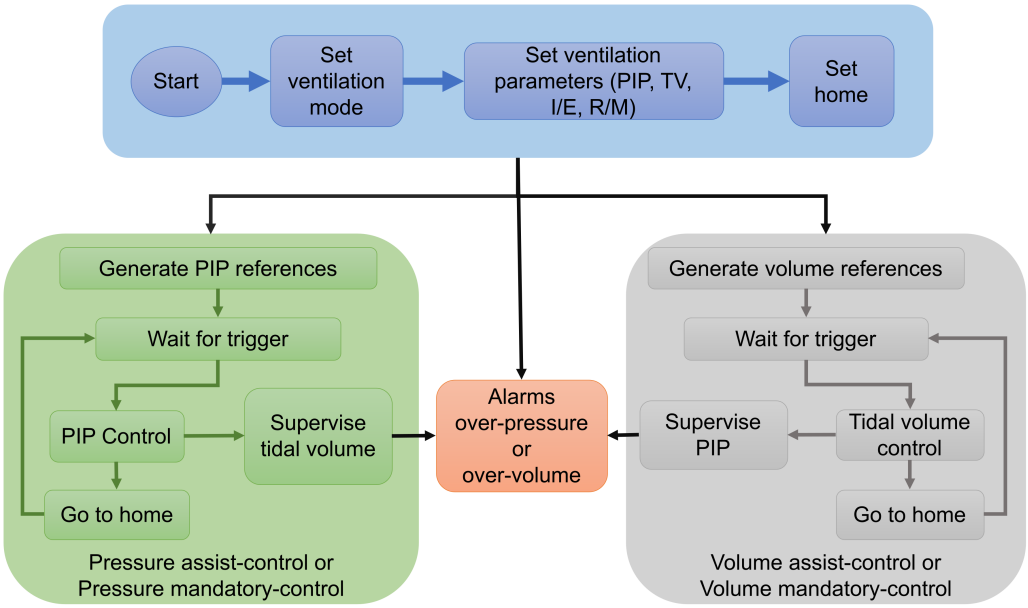

Fig. 3. Finite-State Machine for Mechanical Ventilator.

3 Control Strategies

3.1 Finite-State Machine

The proposed mechanical ventilator includes standard features such as the mandatory ventilation modes with pressure and volume control as well as the capability to slowly discontinue or wean off MV support. To satisfy all the operation modes, a finite-state machine is implemented (Fig. 3). The finite-state machine switches the control and objective to one of three different states. The first state is the setup mode using the operation parameters from the user input interface. The user input interface allows the medical professional to set parameters such as ventilation mode and operation parameters, namely, TV, PIP, RR, and I/E ratio (Table 1). After all ventilation parameters have been defined, the DC geared motor activates forward motion with a low torque reference. This allows the ventilator to set a home position, which ensures that the bag valve has the minimum compression pressure required to hold it in position.

The second state corresponds to one of the two control modes: *pressure control mode* and *volume control mode*. Each mode produces periodic references with set points of PIP and TV. The ventilator includes a trigger system that could start the inspiration process either by the time set in the reference or by a negative inspiratory pressure. The negative inspiratory pressure is used during an assisted mechanical ventilation mode. In this ventilation mode the ventilator monitors the patient respiratory effort and completes the assisted mechanical ventilation. The assisted ventilation mode is a key step into the recover of spontaneous breathing. However, it is important to keep a constant monitoring of the patient breathing to avoid asynchrony between the patient and the MV, which could produce self lung injury [29]. Once the controlled variable has reached the target value, the finite-state machine is activated to switch the controller to a position control, which drives the gearmotor in returning to the home position.

The third state is the alarm activation. In this state, the activated alarm produces a sound that indicates over-pressure or over-volume. In these cases, the medical personnel must check the patient's respiratory conditions and reset the breathing

parameters.

3.2 Active disturbance rejection control

In order to provide robustness to the control of continuous dynamics against unknown model uncertainties and external disturbances, an active disturbance rejection control (ADRC)-based tracking is implemented in this work. ADRC-based tracking has been successfully utilized in the control of other dynamic systems including walking robots [30, 31, 24]. The ADRC-based tracking collects both endogenous disturbances (strap tension loss, manufacturing variability) and exogenous disturbances (external disturbances, breathing irregularity) into a lumped signal referred to as the *total disturbance*. The total disturbance is treated as an unknown, bounded signal with m continuous and bounded derivatives [32]. The core component of the ADRC-based tracking is the design of an extended state observer (ESO) that estimates the total disturbance, which is actively rejected through feedback control [31]. With this approach, the nonlinearities of the system are represented in a simplified model, affine in the control input, with a chain of integrators and the total disturbance. This approach has shown to handle differences between the dynamics of physical mechatronic systems and their mathematical models, driving the tracking errors to small, acceptable values [33, 34].

With the aim to provide robustness to the mechanical ventilator against the uncertainties produced by the variety of the patients' dynamics and the unmodeled dynamic effects of errors from fabrication, assembly, or overuse of portable ventilators, the ADRC approach is proposed as a universal control structure for any mechanical ventilator able to supply continuous gas flow with controlled pressure.

3.2.1 Ventilation dynamic model

A nonlinear morphometric model of the human bronchial tree is utilized to describe the pulmonary functions. This approach divides each bronchial branch and models its dynamics with an equivalent RLC electric circuit [35]. However, this approach results in high-order models with nonlinear, parameters-time-variant dynamics and a wide range of uncertainties [36]. This paper proposes a simplified, equivalent model that uses the Windkessel-based model to describe the pulmonary function dynamics with a reduced number of parameters. This equivalent model reproduces an air chamber with the lungs represented by an elastic reservoir. This approach proposes the use of a well-known RLC electric circuit, (Fig. 4), as an equivalent dynamic model for pressure control mode, which is described as:

$$RF(t) + L\frac{d}{dt}(F(t)) + P_{ins}(t) + \psi(F, P_{ins}, t) = P_{int}(t), \tag{1}$$

satisfying

$$F(t) = C\frac{d}{dt}(P_{ins}(t)), \tag{2}$$

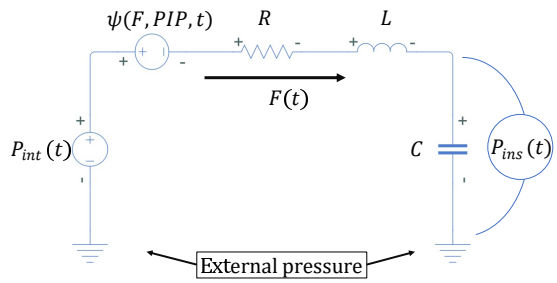

Fig. 4. Electrical analog of pulmonary functions.

where the resistor R represents the air flow resistance, the inductance L represents the chest and lungs inertia, the capacitance C represents the lungs compliance, $F(t)$ is the electrical current that represents the inspiratory air flow, P_{int} is the input voltage for the input pressure, P_{ins} is the output voltage for the inspiratory pressure, and $\psi(F, P_{ins}, t)$ is the unmodel dynamics and the parameter's uncertainties included as input equivalent additive pressure.

Using (1) and (2) the complete model is defined as

$$\begin{aligned} LC\frac{d^2}{dt^2}(P_{ins}(t)) + RC\frac{d}{dt}(P_{ins}(t)) \\ + P_{ins}(t) + \psi(F, P_{ins}, t) = P_{int}(t). \end{aligned} \tag{3}$$

In order to find a dynamic model for the volume control mode, it is possible to use the relation between the inspiratory flow $F(t)$ and the inspitatory volume $V(t)$,

$$F(t) = \frac{d}{dt}(V(t)). \tag{4}$$

Using the time-derivative of (1) with (2) and (4), allows the volume dynamics to be described as

$$\begin{aligned} L\frac{d^3}{dt^3}(V(t)) + R\frac{d^2}{dt^2}(V(t)) + \frac{1}{C}\frac{d}{dt}(V(t)) \\ + \frac{d}{dt}(\psi(F, P_{ins}, t)) = \frac{d}{dt}(P_{int}(t)). \end{aligned} \tag{5}$$

Finally, the integration of (5) with respect to time yields

$$L\frac{d^2}{dt^2}(V(t))+R\frac{d}{dt}(V(t))+\frac{1}{C}V(t) \\ +\psi(F,P_{ins},t)+\rho=P_{int}(t), \tag{6}$$

where ρ is an integration constant.

3.2.2 PIP simplified model

The control objective of the pressure control mode is to drive the mechanical ventilator so that the P_{ins} tracks the setup PIP. In order to achieve such objective, (3) is transformed into the simplified model

$$\frac{d^2}{dt^2}(P_{ins}(t))=\kappa_P P_{int}(t)+\xi_P, \tag{7}$$

where κ_P is the pressure input gain and ξ_P lumps all the uncertainties and unmodel dynamics of the pressure dynamics.

3.2.3 Tidal volume simplified model

The control objective of the volume control mode is to drive the inspitatory volume $V(t)$ to track the reference tidal volume. In order to achieve such objective, (6) is transformed into the simplified model

$$\frac{d^2}{dt^2}(V(t))=\kappa_V P_{int}(t)+\xi_V, \tag{8}$$

where κ_V is the volume input gain and ξ_V lumps all the uncertainties and unmodeled dynamics of the volume dynamics.

3.2.4 Active disturbance rejection control

A universal control structure is proposed for both pressure and volume control ventilation modes. The proposed controller is based on the ADRC approach, which uses an extended state observer (ESO) to perform a feedback control action [37]. Since both ventilation modes (pressure and volume) have dynamic models with the same mathematical structure, the ESO is designed with the same structure, described in detailed below. First, let us define the general model

$$\ddot{y}=\kappa u+\xi, \tag{9}$$

where y is the controlled variable, u is the control input, κ is the input gain, and ξ is a disturbance signal that lumps the effects of unmodeled dynamics, parameter uncertainties, and external disturbances [38]. The general model (9) requires the estimation of the parameter κ. This process could be performed using data acquired from experiments in an test lung and a system identification toolbox [39]. As a remark, it is useful to say that the parameters uncertainties are included into the total disturbance signal ξ.

In order to define a steady-state representation of (9), the lumped disturbance is defined as an state variable of the system such as $\dot{\xi} := h$, where h is a constant input. The steady-state representation of the system is developed by defining the state variables into a state vector, $\mathbf{x} = [x_1 \quad x_2 \quad x_3]^{\mathrm{T}} := [y \quad \dot{y} \quad \xi]^{\mathrm{T}}$. This new representation transforms the general model (9) into

$$\dot{\mathbf{x}} = \begin{bmatrix} 0 & 1 & 0 \\ 0 & 0 & 1 \\ 0 & 0 & 0 \end{bmatrix} \mathbf{x} + \begin{bmatrix} 0 \\ \kappa \\ 0 \end{bmatrix} u + \begin{bmatrix} 0 \\ 0 \\ 1 \end{bmatrix} h, \tag{10}$$

$$y = \begin{bmatrix} 1 & 0 & 0 \end{bmatrix} \mathbf{x}, \tag{11}$$

or in a compact form

$$\dot{\mathbf{x}} = A_{ext}\mathbf{x} + B_{int}u + B_{dis}h, \tag{12}$$

$$y = C\mathbf{x}. \tag{13}$$

Based on the extended model described in (12), a state observer is designed to estimate all the state variables, including the estimation of the disturbance signal that is represented by the state variable x_3. The ESO takes the classical structure of the Luenberger-observer with a virtual system and a correction factor L. This is

$$\dot{\hat{\mathbf{x}}} = A_{ext}\hat{\mathbf{x}} + B_{int}u + L(y - \hat{y}), \tag{14}$$

$$\hat{y} = C\hat{\mathbf{x}}, \tag{15}$$

where $\hat{y}$ is the estimated output. The success of the observer estimating the state variables is essentially defined by the appropriate selection of the matrix L, which can be determined through the computation of the estimation error vector

$\hat{\mathbf{e}} := \mathbf{x} - \hat{\mathbf{x}}$. In order to characterize the $\hat{\mathbf{e}}$ dynamics, let us subtract (14) of (12), so that

$$\dot{\hat{\mathbf{e}}} = (A_{ext} - LC)\hat{\mathbf{e}} + B_{dis}h, \tag{16}$$

which is asymptotically stable if $(A_{ext} - LC)$ is Hurwitz.

Based on the estimated states, a feedback control law is proposed with the following form:

$$u = \frac{1}{\kappa}\left(\ddot{y}^* + k_d(\dot{y}^* - \hat{x}_2) + k_p(y^* - \hat{x}_1) - \hat{x}_3)\right), \tag{17}$$

where y^* is the set point variable, and k_p and k_d are the proportional and derivative gains, respectively.

Finally, the control law (17) is applied to the system represented by the general model (9). This produces an error closed-loop dynamics given by

$$\ddot{e} + k_d\dot{e} + k_p e = \hat{x}_3 - \xi, \tag{18}$$

which is Hurwitz-stable for $k_p, k_d > 0$, and the error, $e := y^* - y$, converges to an upper bounded neighborhood around zero with the bound defined by a small positive value ε, such that

$$|\xi - \hat{x}_3| \leq \varepsilon. \tag{19}$$

In order to avoid an alveoli overpressure (barotrauma) or overdistention (volutrauma) a supervision variable is define as z, with $\bar{z}$ as its maximum permissible value. In the same way, a maximum for the controlled variable is defined as $\bar{y}$. Based on the setup of maximum control and supervision variables, the maximum set point is defined as

$$y^* = \begin{cases} \text{if} \quad (\bar{z} - z) > 0, \text{ then} \quad y^* = \bar{y}, \\ \text{if} \quad (\bar{z} - z) \leq 0, \text{ then} \quad y^* = \bar{y} + k_r(\bar{z} - z), \end{cases} \tag{20}$$

where k_r is a positive constant that allows to reduce the set point variable to avoid the alveoli overpressure or overdistention. Figure 5 shows the block diagram of the complete regulatory control structure.

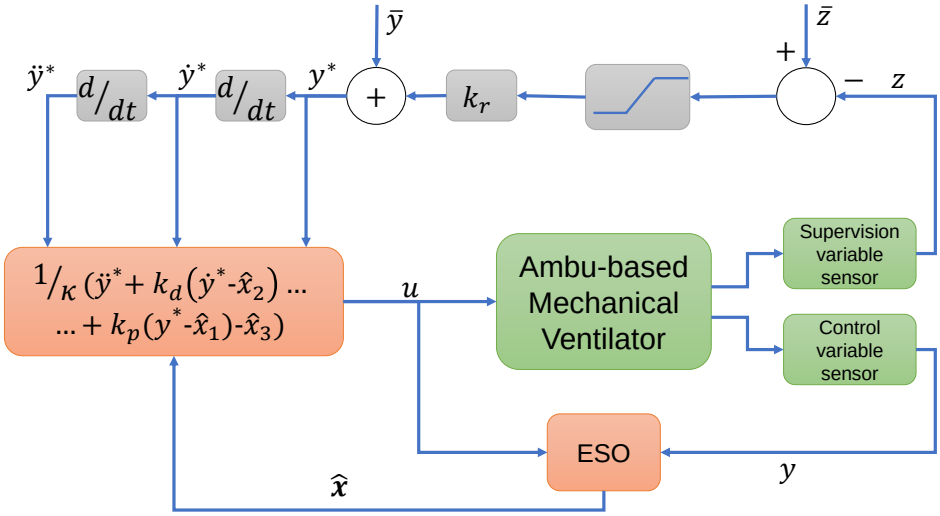

Fig. 5. Regulatory control structure.

4 Experiments

A set of physical experiments of the mechanical ventilator are carried out on a test lung to evaluate the performance of the finite-state machine algorithm on several ventilation modes. The mechanical ventilator is calibrated using a commercial ventilator as the reference. In this case, a Drager, forth generation mechanical ventilator, was used as reference. The behavior of both ventilators was compared with a ventilation setup of PIP 15 cm H2O, RR 15 bpm, and I/E ratio 1:2. The results are presented in the Fig. 6. From the results, the controlled pressure reaches the setup PIP with the target frequency and I/E ratio. The low pressure, PEEP, are setup to 7 and 8 cm H2O for the Drager and our prototype, respectively. The low pressure of our prototype is selected with a PEEP mechanical valve as shown in Fig. 7, where a human-breathing simulator dummy is used to test the complete ventilation system. In emergency conditions, like the produced by the COVID-19, the PEEP valves could be difficult to obtain due to supply chain issues. To alleviate the shortness of these elements, a simple but useful solution is the use of a bucket of water to set PEEP. However, it is important to consider the risk of contamination with sprays produced by the patient exhalation. To avoid contamination in the ICU, it is recommended to incorporate filters into the expiratory hose. An experiment is performed to test our prototype to extreme operating conditions, which includes PIP = 20 cm·H_2O, RR = 30 bpm, I:E = 1:1, and PEEP = 8 cm·H_2O. The results of such experiment are presented in the Fig. 8. It shows that the ventilator achieves the setup parameters; however, noise in the PEEP reading is evidenced.

Parameters uncertainties are ubiquitous in all engineering applications and mechanical ventilators are not an exception. These uncertainties could come out by the variability in the manufacturing process or by the changes in the components properties produced by long term use, e.g., fatigue or strap tension loss. The algorithm proposed in this paper uses the ADRC approach, which allows to reject the effect of model mismatching. In order to show the robustness against parameters uncertainties and the reliability of the prototype, a set of experiments is performed with three different PIP settings (10, 15, 20 cm $\cdot$ H_2O). The results of such experiments are shown in the Figure 9, where is evident the pressure variation in different breathing cycles with its central mean and the shadow produced by the deviation in the measurement. The maximum standard

deviation of the pressure measurement for the experiments with PIP settings of 10, 15, and 20 cm $\cdot$ H_2O are 0.5703, 1.6442, and 3.0053, respectively.

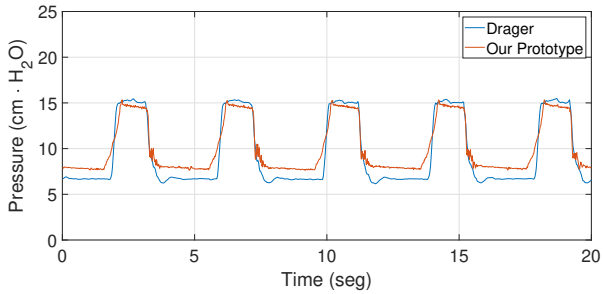

Fig. 6. Pressures comparison between a commercial ventilator and our prototype.

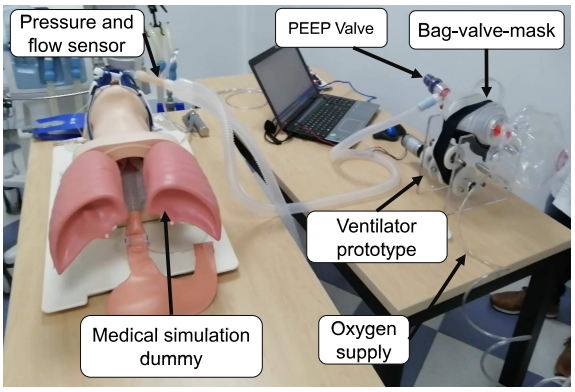

Fig. 7. Human-breathing simulation test.

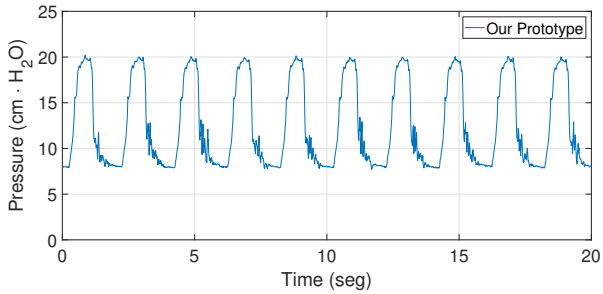

Fig. 8. Our prototype with PIP = 20 cm$\cdot$$H_2O$, RR = 30 bpm, I:E = 1:1, and PEEP = 8 cm$\cdot$$H_2O$.

5 Conclusion and Final Remarks

A functional prototype of a portable bag valve-based mechanical ventilator has been designed, fabricated, and tested. The ventilator uses a strap to compress the bag and deliver oxygen to the patient. Carbon dioxide is cleared from the patient

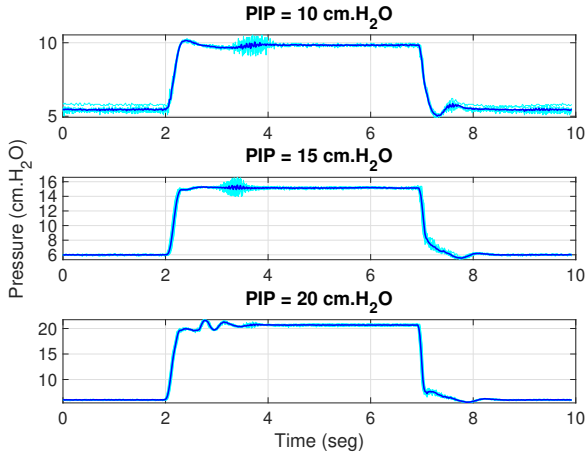

Fig. 9. Breathing cycles and their mean behavior for RR = 6 bpm, I:E = 1:1, and PEEP = 6 cm·H_2O .

while maintaining a positive end-expiratory pressure (PEEP) and the expiratory circuit. The motion of the strap and the resulting compression of the bag valve are controlled by a geared DC motor. The tidal volume (TV), peak inspiration pressure (PIP), respiratory rate (RR), and inspiratory/expiratory time ratio (I/E ratio) can be set and controlled using a closed-loop control system.

The active disturbance rejection control (ADRC) algorithm makes the ventilator robust to external and internal perturbations. External perturbations include misalignment, loss of tension in the strap, strap slipping, and fabrication errors. Internal perturbations include breathing irregularities and random events during the operation. The ADRC approach was proposed as a universal control structure for the bag valve-based or any mechanical ventilator able to supply continuous air flow with controlled pressure. The same ADRC structure is used ether for pressure or volume control. While measurable pressure and volume can reflect the stresses and strains on the lung tissue induced by the mechanical ventilation, further analysis of the exhaled gas, blood gas analysis, and lung imaging are recommended to better inform clinicians of the appropriateness of the ventilation [40]. An adequate monitoring of the lung mechanical function during the mechanical ventilation provides a feedback signal to adequately set ventilation parameters and minimize ventilator-induced lung injury (VILI) [20, 21].

The cost of the physical prototype is abut $425, including all structural elements, actuators, and control hardware components. The total number of mechanical parts is 23 and the overall dimension is $25\times25\times25$ cm and the total weight is 3.5 kg. A more compact and lighter design with fewer parts is possible by consolidating flat panels and spacers with more complex but fewer plastic shapes.

Most errors that a trained clinician could make when using this equipment are not specific to this mechanical ventilator design. These include errors associated with settings, ventilation mode, and patient tubing [41]. Specific errors may be related with valve bag strapping, but these have not been thoroughly investigated. Preliminary results of laboratory testing on a test lung demonstrate a successful operation of the ventilator demonstrating rejection of model uncertainties and external disturbances. A long-term cycling test is under way to evaluate the effect of fatigue load on bag valve, the strap attachment, and other mechanical components. The results of these test will inform about possible design modifications. In addition, the design of an external enclosure would be recommended protect the ventilator from the work environment. The prototype

is undergoing clinical tests and has not yet been approved for use in patients. No tests in animals or humans have been conducted.

Acknowledgment

The authors would like to thank a large number of health practitioners, researchers, and engineers who have shared their experience. Among them, we would like to specially thank the COVID19-Crisis Colombia team and ISOMEC manufacturer.

This research was supported by the Office of Research at the Universidad de San Buenaventura, Bogota campus, the Office of Research at the Universidad Nacional de Colombia, Bogota campus, and the National Science Foundation NRT-IGE grant 1633426.

References

[1] Mackenzie, I., 2008. *Core Topics in Mechanical Ventilation*. Cambridge Medicine. Cambridge University Press.

[2] Metnitz, P. G., Metnitz, B., Moreno, R. P., Bauer, P., Sorbo, L. D., Hoermann, C., Carvalho, S. A. D., and Ranieri, V. M., 2009. "Epidemiology of mechanical ventilation: Analysis of the SAPS 3 database". *Intensive Care Medicine,* **35**, p. 816–825.

[3] Wunsch, H., Linde-Zwirble, W. T., Angus, D. C., Hartman, M. E., Milbrandt, E. B., and Kahn, J. M., 2010. "The epidemiology of mechanical ventilation use in the United States". *Critical Care Medicine,* **38**, p. 1947–1953.

[4] The American Association for the Surgery Trauma. Mechanical ventilation in the intensive care unit.

[5] Centers for Disease Control and Prevention (CDC). Coronavirus Disease 2019 (COVID-19). Cases in the U.S.

[6] L., M. C. A., and I., M. J., 2017. "Ventilation, ventilator management". *StatPearls Publishing,* **6**, p. 6.

[7] Mortelliti, M. P., and Manning, H. L., 2002. "Acute respiratory distress syndrome". *American Family Physician,* **65**, p. 1823–1830.

[8] Amitai, A., Sinert, R. H., Regan, A., and Jain, A., 2020. Ventilator management, Apr.

[9] Davidson, A. C., Banham, S., Elliott, M., Kennedy, D., Gelder, C., Glossop, A., Church, A. C., Creagh-Brown, B., Dodd, J. W., Felton, T., Foëx, B., Mansfield, L., McDonnell, L., Parker, R., Patterson, C. M., Sovani, M., and Thomas, L., 2016. "BTS/ICS guideline for the ventilatory management of acute hypercapnic respiratory failure in adults". *Thorax,* **71**(Suppl 2), pp. ii1–ii35.

[10] Dreyfuss, D., Soler, P., Basset, G., and Saumon, G., 1988. "High inflation pressure pulmonary edema: respective effects of high airway pressure, high tidal volume, and positive end-expiratory pressure". *The American review of respiratory disease,* **137**(5), pp. 1159–1164.

[11] Warner, M. A., and Patel, B., 2013. "Mechanical Ventilation". In *Benumof and Hagberg's Airway Management*, C. A. Hagberg, ed., 3rd ed. W.B. Saunders, Philadelphia, pp. 981–997.

[12] Müller, G. V., 2020. "Hersteller von beatmungsgeräten produzieren massiv mehr, aber können die nachfrage trotzdem nicht decken". *Neue Zürcher Zeitung*, Mar.

[13] Mathanlal, T., Israel Nazarious, M., Mantas-Nakhai, R., Zorzano, M.-P., and Martin-Torres, J., 2020. "Atmo-vent: An adapted breathing atmosphere for covid-19 patients". *HardwareX,* **8**, pp. e145–e169.

[14] Al Husseini, A. M., Lee, H. J., Negrete, J., Powelson, S., Servi, A. T., Slocum, A. H., and Saukkonen, J., 2010. "Design and prototyping of a low-cost portable mechanical ventilator". *Transactions of the ASME-W-Journal of Medical Devices,* **4**(2), p. 027514.

[15] Petsiuk, A., Tanikella, N. G., Dertinger, S., Pringle, A., Oberloier, S., and Pearce, J. M., 2020. "Partially reprapable automated open source bag valve mask-based ventilator". *HardwareX,* **8**, pp. e131–e158.

[16] Gattinoni, L., Quintel, M., and Marini, J. J., 2018. Volutrauma and atelectrauma: which is worse?

[17] McGuinness, G., Zhan, C., Rosenberg, N., Azour, L., Wickstrom, M., Mason, D. M., Thomas, K. M., and Moore, W. H., 2020. "Increased incidence of barotrauma in patients with covid-19 on invasive mechanical ventilation". *Radiology,* **297**(2), pp. E252–E262.

[18] Bates, J. H., Gaver, D. P., Habashi, N. M., and Nieman, G. F., 2020. "Atelectrauma versus volutrauma: A tale of two time-constants". *Critical care explorations,* **2**(12).

[19] Cipulli, F., Vasques, F., Duscio, E., Romitti, F., Quintel, M., and Gattinoni, L., 2018. "Atelectrauma or volutrauma: the dilemma". *Journal of thoracic disease,* **10**(3), p. 1258.

[20] Bates, J. H., and Smith, B. J., 2018. "Ventilator-induced lung injury and lung mechanics". *Annals of translational medicine,* **6**(19).

[21] Mori, V., Smith, B. J., Suki, B., and Bates, J. H., 2020. "Modeling lung derecruitment in vili due to fluid-occlusion: The role of emergent behavior". *Frontiers in physiology,* **11**, p. 1402.

[22] Gattinoni, L., 2016. "Ultra-protective ventilation and hypoxemia". *Critical Care,* **20**(1), pp. 1–2.

[23] Gattinoni, L., Quintel, M., and Marini, J. J., 2020. ""less is more" in mechanical ventilation.". *Intensive Care Med*, pp. 780–782.

[24] Arcos-Legarda, J., Cortes-Romero, J., Beltran-Pulido, A., and Tovar, A., 2019. "Hybrid disturbance rejection control of dynamic bipedal robots". *Multibody System Dynamics,* **46**(3), pp. 281–306.

[25] Islam, M. R., Ahmad, M., Hossain, M. S., Muinul Islam, M., and Uddin Ahmed, S. F., 2019. "Designing an electromechanical ventilator based on double cam integration mechanism". In 2019 1st International Conference on Advances in Science, Engineering and Robotics Technology (ICASERT), pp. 1–6.

[26] Acho, L., Vargas, A. N., and Pujol-Vázquez, G., 2020. "Low-cost, open-source mechanical ventilator with pulmonary monitoring for covid-19 patients". In Actuators, Vol. 9, Multidisciplinary Digital Publishing Institute, p. 84.

[27] Rice University. ApolloBVM - Emergency Use Ventilator.

[28] Massachusetts Institute of Technology. MIT Emergency Ventilator (E-Vent) Project.

[29] Bertoni, M., Spadaro, S., and Goligher, E. C., 2020. "Monitoring patient respiratory effort during mechanical ventilation: lung and diaphragm-protective ventilation". *Annual Update in Intensive Care and Emergency Medicine 2020*, pp. 21–35.

[30] Gao, Z., 2014. "On the centrality of disturbance rejection in automatic control". *ISA transactions,* **53**(4), pp. 850–857.

[31] Huang, Y., and Xue, W., 2014. "Active disturbance rejection control: methodology and theoretical analysis". *ISA transactions,* **53**(4), pp. 963–976.

[32] Sira-Ramírez, H., Gao, Z., and Canuto, E., 2014. "An active disturbance rejection control approach for decentralized tracking in interconnected systems". In Control Conference (ECC), 2014 European, IEEE, pp. 588–593.

[33] Guo, B.-Z., and Zhao, Z.-L., 2016. *Active Disturbance Rejection Control for Nonlinear Systems: An Introduction*. John Wiley & Sons.

[34] Arcos-Legarda, J., Cortes-Romero, J., and Tovar, A., 2016. "Active disturbance rejection control based on generalized proportional integral observer to control a bipedal robot with five degrees of freedom". In American Control Conference (ACC), 2016, IEEE.

[35] Barbini, P., Brighenti, C., Cevenini, G., and Gnudi, G., 2005. "A dynamic morphometric model of the normal lung for studying expiratory flow limitation in mechanical ventilation". *Annals of biomedical engineering,* **33**(4), pp. 518–530.

[36] Lee, R.-M., and Tsai, N.-C., 2013. "Dynamic model of integrated cardiovascular and respiratory systems". *Mathematical Methods in the Applied Sciences,* **36**(16), pp. 2224–2236.

[37] Sira-Ramírez, H., Luviano-Juárez, A., Ramírez-Neria, M., and Zurita-Bustamante, E. W., 2018. *Active disturbance rejection control of dynamic systems: a flatness based approach*. Butterworth-Heinemann.

[38] Beltran, L. M., Garzon-Castro, C. L., Garces, F., and Moreno, M., 2012. "Monitoring and control system used in microalgae crop". *IEEE Latin America Transactions,* **10**(4), pp. 1993–1998.

[39] Ljung, L., 1999. "System identification". *Wiley encyclopedia of electrical and electronics engineering*, pp. 1–19.

[40] Larsson, A., and Guerin, C., 2017. "Monitoring of lung function in acute respiratory distress syndrome". *Annals of translational medicine,* **5**(14).

[41] Williams, L., and Sharma, S., 2020. *Ventilator Safety*. StatPearls Publishing.

A Bill of Materials of the Mechanical Ventilator

Table 2. Mechanical ventilator's parts.

Item number	Quantity	Name	Material
1	1	Lateral Press 1	Polyglass
2*	2	Spacer	Stainless steel,304
3	1	Ambu bag	N/A
4	1	Pivot spacer	Stainless steel,304
5	1	Pivot	Polypropylene, general purpose
6	4	Bearing W6001-2RS1	N/A
7*	2	Centering	Polypropylene, general purpose
8	3	Bearing end	Polyglass
9	1	Axis 1	Stainless steel,304
10	1	Traction	Polypropylene, general purpose
11	1	Lateral Press 2	Polyglass
12	1	Strap	N/A
13	2	Pin	Stainless steel,304
14	1	Ambu base	Stainless steel,304
15	1	Motor base	Polypropylene, general purpose
16	1	Motor coupling	Stainless steel,304
17	18	Flat washer M6x12	Stainless steel,304s
18	18	Hex socket cylindrical M6x25	Stainless steel,304
19	12	Hex nut autolock M6	Stainless steel,304
20	4	Pin seger 12mm	Steel
21*	2	Hex socket screw M4x8	Steel
22	1	DC Gearmotor	N/A
23*	1	Encoder	N/A

*Unballoned item.

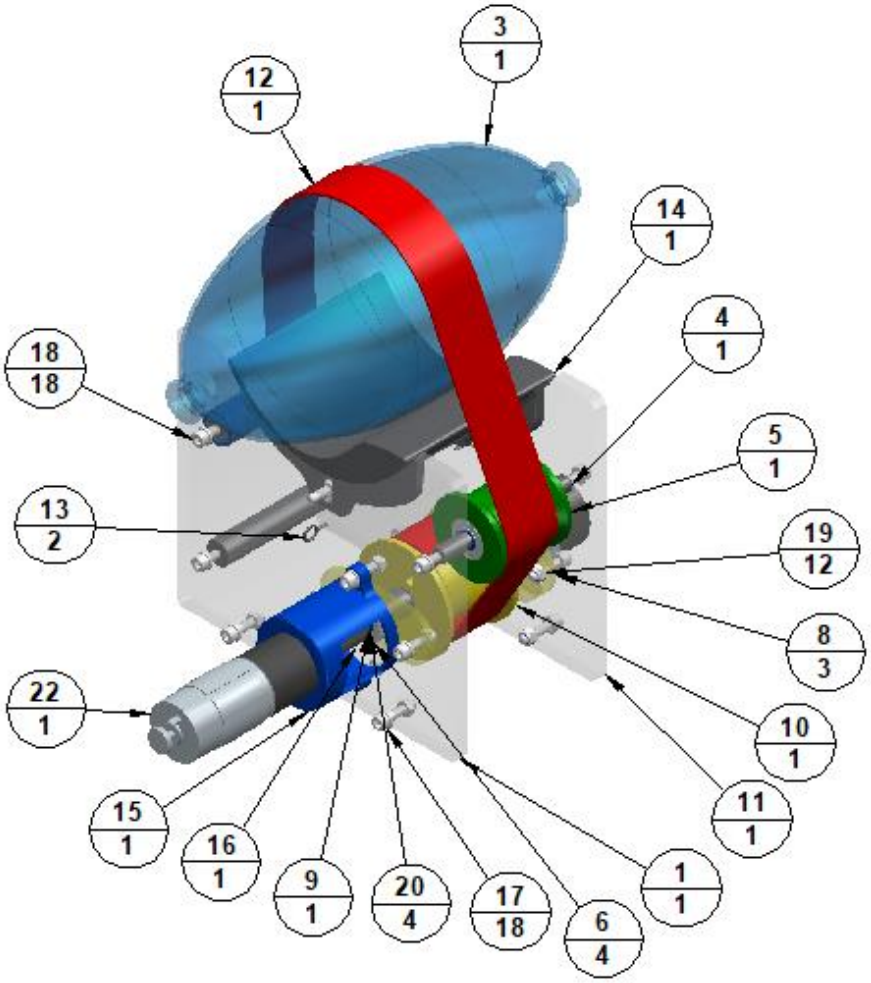

Fig. 10. Mechanical ventilator parts.

List of Figures

List of Tables